AIAA JOURNAL
Vol. 42, No. 10, October 2004

Technical Notes

TECHNICAL NOTES are short manuscripts describing new developments or important results of a preliminary nature. These Notes cannot exceed six manuscript pages and three figures; a page of text may be substituted for a figure and vice versa. After informal review by the editors, they may be published within a few months of the date of receipt. Style requirements are the same as for regular contributions (see inside back cover).

Simple Method for Generating Inflow Turbulence

Z. Xiong,* S. Nagarajan,† and S. K. Lele‡
Stanford University, Stanford, California 94305

Introduction

THE phenomenal increase in computational power and improvements in numerical methods have brought spatially evolving turbulent flows under computational scrutiny. This class of flows involves a mean stream carrying turbulence into the domain of interest (class II.2.1 in Hunt and Carruthers[1]). In the direct numerical simulations and large-eddy simulations (LES) of such problems, a convecting turbulent stream needs to be imposed in the form of an inflow boundary condition. One option is to specify an artificial turbulent field at the inflow[2–4] and allow it to develop into realistic turbulence inside the domain before it interacts with bodies and/or undergoes changes that are to be studied. However, in some cases (e.g., simulations of flow over a bluff body with a C or O mesh), the associated cost is prohibitive as the grid might not be easily extended to include such a development zone. The second option is to carry out a separate simulation, which acts as the development zone, and impose the resulting realistic turbulent field at the inflow boundary. The method described herein follows the second approach for generating long time sequences of realistic turbulence that can be specified at the inflow boundary.

We consider compressible turbulent flow in an arbitrary domain with a nominally uniform mean flow. The coordinate system (x, y, z) is such that the mean stream is aligned with the x axis. The incoming flow is assumed to consist of a "frozen" turbulent field being convected by the mean across the inflow boundary. The time-varying boundary condition can then be obtained from the frozen turbulent field by converting, through Taylor's hypothesis, the x coordinate to time.[2] The problem of providing inflow turbulence then reduces to an accurate description of the frozen field. The simplest approach is to obtain a realistic field of turbulent flow, with desired characteristics (Reynolds number, length scale, intensity etc.), from a separate calculation. However, this approach can turn out to be very expensive. For example, in the freestream turbulence (FST)-induced bypass transition of a boundary layer, statistical convergence requires at least 10 flow-through times, making the inflow turbulence calculation 10 times larger than the problem of interest. This limitation can be overcome by catenating, in random order, turbulence in smaller boxes provided that the catenation is carried out without significant modification of turbulence characteristics. Exploiting isotropy, if present, and reusing individual boxes, a long time record can be generated with a limited number of realizations. Compared to the brute-force method of simulating a long box of turbulence with the required characteristics, this procedure is not only cheaper but is also capable of generating inflow turbulence with time-varying characteristics. This can be achieved by slowly varying the properties of turbulence from one box to the next, which is not possible if a single box is used. In the rest of this Note, we only consider homogeneous isotropic freestream turbulence, which covers a large class of problems that involve grid-generated turbulence. However, the method used herein can be easily extended to other types of disturbances such as sheared turbulence.

Combination of Velocity Fields

Consider two independent, identically distributed (iid) random velocity fields $\boldsymbol{u}^{(1)}$ and $\boldsymbol{u}^{(2)}$. Let $\boldsymbol{u}$ be a linear combination of the form

$$\boldsymbol{u} = \alpha \boldsymbol{u}^{(1)} + \beta \boldsymbol{u}^{(2)} \tag{1}$$

where α and β are scalar constants. If $\boldsymbol{u}^{(1)}$ and $\boldsymbol{u}^{(2)}$ are velocity fields corresponding to homogeneous isotropic turbulence, their mean is zero, as is that of the new field $\boldsymbol{u}$. Furthermore, the two-point correlation $R_{ij}(\boldsymbol{r})$ for the new field $\boldsymbol{u}$,

$$\begin{aligned} R_{ij}(\boldsymbol{r}) = \langle u_i(\boldsymbol{x}) u_j(\boldsymbol{x}+\boldsymbol{r}) \rangle &= \alpha^2 \left\langle u_i^{(1)}(\boldsymbol{x}) u_j^{(1)}(\boldsymbol{x}+\boldsymbol{r}) \right\rangle \\ &+ \beta^2 \left\langle u_i^{(2)}(\boldsymbol{x}) u_j^{(2)}(\boldsymbol{x}+\boldsymbol{r}) \right\rangle \\ &+ \alpha\beta \left[\left\langle u_i^{(1)}(\boldsymbol{x}) u_j^{(2)}(\boldsymbol{x}+\boldsymbol{r}) \right\rangle + \left\langle u_i^{(2)}(\boldsymbol{x}) u_j^{(1)}(\boldsymbol{x}+\boldsymbol{r}) \right\rangle \right] \end{aligned} \tag{2}$$

reduces to

$$R_{ij}(\boldsymbol{r}) = (\alpha^2 + \beta^2) R_{ij}^{(1)} \tag{3}$$

by virtue of $\boldsymbol{u}^{(1)}$ and $\boldsymbol{u}^{(2)}$ being iid, where the angled brackets $\langle\rangle$ indicate an averaging (volume average suffices for the homogeneous fields under consideration). To retain the second-order statistics of the original fields $\boldsymbol{u}^{(1)}$ and $\boldsymbol{u}^{(2)}$, an appropriate rescaling of the definition in Eq. (1) is required. This renormalization yields

$$\boldsymbol{u} = \alpha \Big/ \sqrt{\alpha^2 + \beta^2}\, \boldsymbol{u}^{(1)} + \beta \Big/ \sqrt{\alpha^2 + \beta^2}\, \boldsymbol{u}^{(2)} \tag{4}$$

Using trigonometric identities, this can be rewritten as

$$\boldsymbol{u} = \cos\theta\, \boldsymbol{u}^{(1)} + \sin\theta\, \boldsymbol{u}^{(2)} \tag{5}$$

The new field so obtained retains the zero mean value and second-order statistics of the original fields. This linear combination can be generalized by smoothly varying θ from one field to another over a blending zone. As shown in Fig. 1a, θ is increased from 0 to $\pi/2$ in the blending zone. With $\theta = \theta(x)$ and $\langle\,\rangle$ restricted to averaging in $y-z$ plane, the single-point statistics are preserved, as are two-point correlations in the $y-z$ plane. However, along the blending coordinate (x direction), the two-point statistics are modified. The extent

Received 30 October 2003; revision received 13 May 2004; accepted for publication 25 May 2004.

*Research Assistant, Department of Mechanical Engineering; currently Postdoctoral Fellow, Fusion Energy Program, Lawrence Livermore National Laboratory, Livermore, CA 94550-9234.

†Research Assistant, Department of Mechanical Engineering; currently Postdoctoral Fellow, Department of Mechanical Engineering.

‡Professor, Department of Mechanical Engineering; also Professor, Department of Aeronautics and Astronautics. Member AIAA.

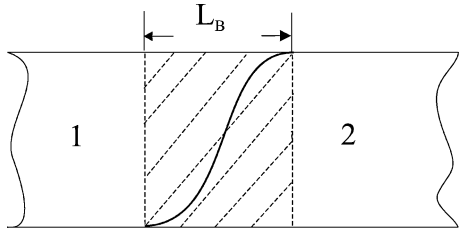

Fig. 1a Blending function (——) $0 < \theta(x) < \pi/2$ for joining two turbulence realizations.

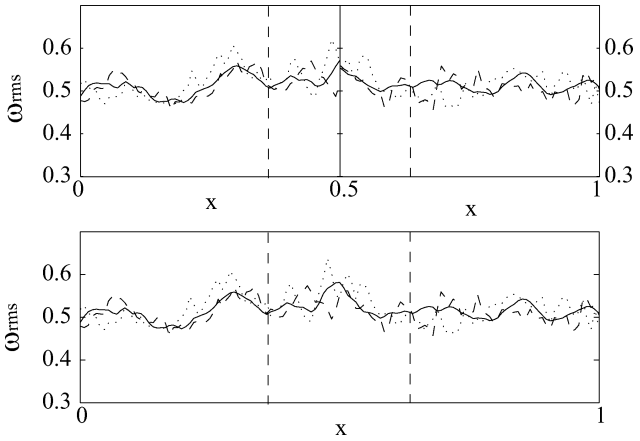

Fig. 1b Turbulent vorticity fluctuation before and after blending. For clarity, the second half of the first data set and the first half of the second data set are shown together on top. The blended data of the corresponding range are shown at the bottom: ——, – – –, and · · · ·, ω in x, y, z directions, respectively. The blending zones are marked between dashed lines in both graphs.

of this modification can be estimated by considering the following two-point correlation:

$$\langle u_i(\boldsymbol{x}) u_j(\boldsymbol{x}+\boldsymbol{r})\rangle = \left\langle \left[\cos(\theta) u_i^{(1)} + \sin(\theta) u_i^{(2)}\right] \times \left[\cos(\theta+\phi) u_j^{(1)} + \sin(\theta+\phi) u_j^{(2)}\right]\right\rangle \tag{6}$$

where $\phi(x, r_1) = \theta(x + r_1) - \theta(x)$. Because $\boldsymbol{u}^{(1)}$ and $\boldsymbol{u}^{(2)}$ are independent, Eq. (6) reduces to

$$\langle u_i(\boldsymbol{x}) u_j(\boldsymbol{x}+\boldsymbol{r})\rangle = [\cos(\theta)\cos(\theta+\phi) + \sin(\theta)\sin(\theta+\phi)] \times R_{ij}(\boldsymbol{r}) = \cos(\phi) R_{ij}(\boldsymbol{r}) \tag{7}$$

The two-point correlation in the blended field is therefore lower than the original fields by a factor of $\cos(\phi)$. Expanding $\theta(x + r)$ using Taylor's series about x and using the series expansion for $\cos(\phi)$, this reduces to

$$\langle u_i(\boldsymbol{x}) u_j(\boldsymbol{x}+\boldsymbol{r})\rangle = \left[1 - \frac{1}{2}\left(r_1 \frac{\mathrm{d}\theta}{\mathrm{d}x}\right)^2 + \cdots\right] R_{ij}(\boldsymbol{r}) \tag{8}$$

From this expression, an estimate for the size of the blending zone can be obtained. Requiring that the two-point correlation between points separated by one integral length scale $r_1 = \mathcal{L}$ in the x direction is not to change by more than ϵ, this yields an estimate for the gradient $(\mathrm{d}\theta/\mathrm{d}x)_{\max}$ as

$$\left(\frac{\mathrm{d}\theta}{\mathrm{d}x}\right)_{\max} < \frac{\sqrt{2\epsilon}}{\mathcal{L}} \tag{9}$$

which can be used to determine the blending length L_B as

$$L_B \sim \frac{\pi/2}{(\mathrm{d}\theta/\mathrm{d}x)_{\max}} \sim \frac{\pi}{2\sqrt{2\epsilon}}\mathcal{L} \tag{10}$$

This expression indicates that the blending length L_B has to be large to minimize the modification of the two-point correlation in the x direction by the blending procedure.

The dependence of θ on x within the blending zone also introduces an extra term $\mathcal{D}_e$ in the dilatation field:

$$\nabla \cdot \boldsymbol{u} = \cos(\theta)\left[\nabla \cdot \boldsymbol{u}^{(1)}\right] + \sin(\theta)\left[\nabla \cdot \boldsymbol{u}^{(2)}\right] + \mathcal{D}_e$$

$$\mathcal{D}_e = \left[-\sin(\theta)\,\boldsymbol{u}^{(1)} + \cos(\theta)\,\boldsymbol{u}^{(2)}\right]\frac{\mathrm{d}\theta}{\mathrm{d}x} \tag{11}$$

In incompressible flows, $\mathcal{D}_e$ violates mass conservation, whereas in compressible flows it can cause large artificial pressure fluctuations. This undesired dilatation can be removed by a projection method based on the Helmholtz decomposition theorem for the velocity vector $\boldsymbol{u}$

$$\boldsymbol{u} = \nabla \times \boldsymbol{A} + \nabla\varphi \tag{12}$$

where $\boldsymbol{A}$ and φ are the vector and scalar potential of $\boldsymbol{u}$. The scalar potential φ_e corresponding to the extra dilatation $\mathcal{D}_e$ satisfies a Poisson equation obtained by taking the divergence of Eq. (5):

$$\nabla^2 \varphi_e = \mathcal{D}_e \tag{13}$$

This equation is solved with homogeneous boundary conditions in the x direction and periodic in the other two directions. Subtracting $\nabla\varphi_e$ from $\boldsymbol{u}$ yields the final expression of the blended velocity $\tilde{\boldsymbol{u}}$ as

$$\tilde{\boldsymbol{u}} = \boldsymbol{u} - \nabla\varphi_e \tag{14}$$

Application

Two sample data sets of decaying homogeneous isotropic turbulence are used to demonstrate the blending procedure. These fields are obtained through LES in a rectangular box of aspect ratio 4:4:1. The filtered compressible Navier–Stokes equations are solved using sixth-order compact finite difference scheme and fourth-order Runge–Kutta time integration. The dynamic model,[5] with Simpson's rule as the test filter, is used to approximate the subgrid terms. The Reynolds number based on the integral length scale and rms value of velocity fluctuation is 240, and the number of grid points is $128 \times 128 \times 32$. The two simulations are initialized with solenoidal velocity fields having the same energy spectrum but independent phase relationships. After the turbulence statistics such as intensity and length scale reach predetermined values, a snapshot of each flowfield is taken. The two data sets can be regarded as different realizations of the same turbulent statistical state, to which the preceding blending procedure is applied. In general, the blending zone should be kept small compared to the box length to minimize modifications to the original data sets. On the other hand, as shown in Eq. (10), the blending zone has to be long for the change in second-order statistics in the x direction to be small. As a compromise, the size of the blending zone is taken as $\frac{1}{8}$ of the box length. The results for blending over 1/16 of the box length are found to be similar. The turbulent vorticity distribution, plotted in Fig. 1b before and after blending, shows the smoothness of the blending.

As a real example, the blending procedure is used in LES of freestream turbulence induced heat-transfer enhancement at a turbine blade leading edge. This simulation uses fourth-order finite difference and fully implicit time-marching schemes.[6,7] Twelve different realizations of homogeneous isotropic turbulence with intensity $Tu = 5\%$ and integral length scale $\mathcal{L}/D = 0.1$ are precomputed, lined up spatially, and joined together by applying the blending procedure at the interface between consequent fields. The result is a box of turbulence 12 times longer than each individual realization, but with the same characteristics as each one. The FST so produced impinges upon an elliptic leading edge of an isothermal flat plate from $1.5D$ upstream. The distribution of the averaged Frössling number

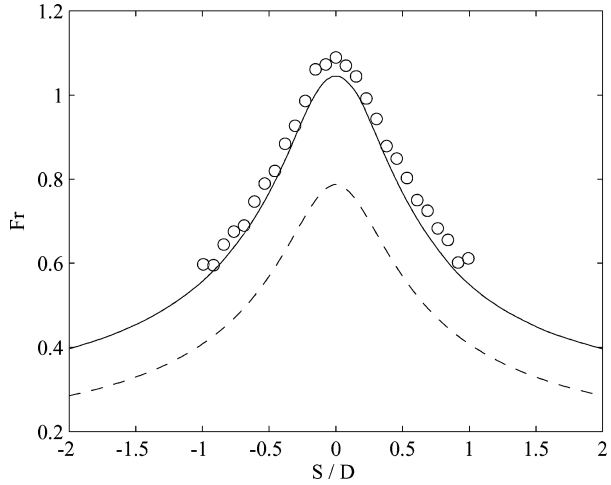

Fig. 2 Distribution of averaged Frössling number along the surface: ——, LES with FST; – – –, laminar value without FST; and ○, experiments by Van Fossen et al.[8] Turbulence intensity is 5% and integral length scale 0.1 *D*.

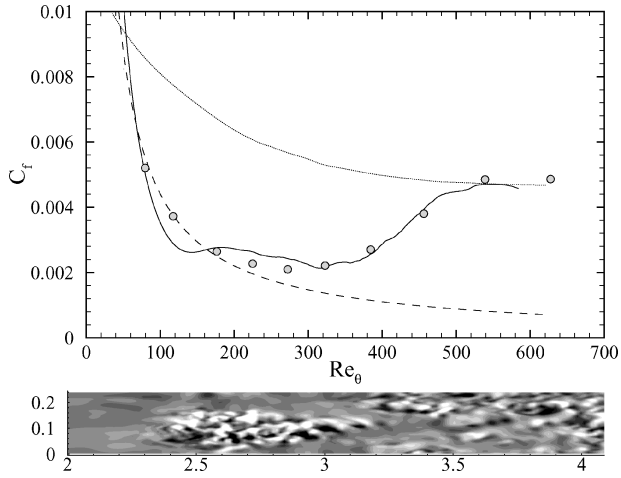

Fig. 3 Development of skin-friction coefficient along the flat plate with momentum thickness Reynolds number Re_θ: ——, simulation result; – – – and · · · ·, laminar and turbulent values; and ○, experimental results of Roach and Brierley[11] case T3A. Lower figure is a plan view of spanwise velocity contours showing bypass transition. Note the turbulent spot centered around $x \sim 2.6$ and a fully turbulent region downstream of $x \sim 3.75$.

$Fr = Nu/\sqrt{(Re)}$ on the surface is compared against experimental measurements[8] in Fig. 2, where Reynolds number Re is based on the inflow velocity U and the leading-edge diameter D, and Nu is the Nusselt number. Both the computation and experimental results show that the surface distribution of the heat-transfer coefficient is essentially the same as in the laminar case, but its amplitude is significantly increased by the freestream turbulence. The LES result is slightly lower than the experimental measurements as not all of the turbulence scales are resolved in the computation. Furthermore, this procedure has also been successfully applied in LES of bypass transition as a result of freestream turbulence.[9] This simulation uses compact staggered schemes[10] implemented and validated in curvilinear coordinates. In this case, a flat plate with a superellipse leading edge of aspect ratio 10 is subjected to FST of intensity $Tu = 3.3\%$. The integral length scale of FST is of the same order as the leading-edge diameter D and the Reynolds number $Re = UD/\nu = 3 \times 10^3$. The inflow boundary is placed $7.5D$ from the leading edge. The plot of skin-friction coefficient shown in Fig. 3 shows good agreement with the the experiments of Roach and Brierley.[11] The onset of transition in both cases is around $Re_\theta \sim 300$, and transition is completed by $Re_\theta \sim 550$. The simulation lies below the Blasius value for $Re_\theta < 140$ as this corresponds to the adverse pressure gradient region of the leading edge. Contours of spanwise velocity fluctuation in the boundary layer, also shown in Fig. 3, show a turbulent spot followed by a fully turbulent boundary layer.

Conclusions

A blending procedure is described for combining realizations of homogeneous isotropic turbulence into a unified field that serves as a realistic representation of freestream turbulence. Different realizations are catenated by a smooth blending function, and extra dilatation is removed using Helmholtz vector decomposition theorem. The combined field preserves the turbulence intensity, and the change to other statistical quantities are shown to be minimal. This simple yet effective method could be useful in other direct or large eddy simulations in which effects of sustained freesteam turbulence are important.

Acknowledgments

This work is supported by the Air Force Office of Scientific Research under Grant F94620-01-1-0138 with. Tom Beutner as the Program Manager. The computer resources were provided by the Defense University Research Instrumentation Program Beowulf cluster under Grant F49620-01-1-0239 and by U.S. Department of Defense parallel computers at the U.S. Army Research Laboratory.

References

[1]Hunt, J. C. R., and Carruthers, D. J., "Rapid Distortion Theory and the 'Problem' of Turbulence," *Journal of Fluid Mechanics,* Vol. 212, 1990, pp. 497–532.

[2]Lee, S. S., Lele, S. K., and Moin, P., "Simulation of Spatially Evolving Compressible Turbulence and the Application of Taylor's Hypothesis," *Physics of Fluids A,* Vol. 4, No. 7, 1992, pp. 1521–1530.

[3]Klein, M., Sadiki, A., and Janicka, J., "A Digital Filter Based Generation of Inflow Data for Spatially Developing Direct Numerical or Large Eddy Simulations," *Journal of Computational Physics,* Vol. 186, No. 2, 2003, pp. 652–665.

[4]Glaze, D. J., and Frankel, S. H., "Stochastic Inlet Conditions for Large-Eddy Simulation of a Fully Turbulent Jet," *AIAA Journal,* Vol. 41, No. 6, 2003, pp. 1064–1072.

[5]Moin, P., Squires, K., Cabot, W., and Lee, S., "A Dynamic Subgrid-Scale Model for Compressible Turbulence and Scalar Transport," *Physics of Fluids A,* Vol. 3, No. 11, 1991, pp. 2746–2757.

[6]Xiong, Z., and Lele, S. K., "2003 Simulation and Analysis of Stagnation Point Heat Transfer Under Free-Stream Turbulence," AIAA Paper 2003-1259, Jan. 2003.

[7]Xiong, Z., "Stagnation Point Flow and Heat Transfer Under Free-Stream Turbulence," Ph.D. Dissertation, Dept. of Mechanical Engineering, Stanford Univ., Stanford, CA, Aug. 2004.

[8]Van Fossen, G. J., Simoneau, R. J., and Ching, C. Y., "Influence of Turbulence Parameters, Reynolds Number and Body Shape on Stagnation Region Heat Transfer," *Journal of Heat Transfer*, Vol. 117, No. 3, 1995, pp. 593–603.

[9]Nagarajan, S., "Leading-Edge Effects in Bypass Transition," Ph.D. Dissertation, Dept. of Mechanical Engineering, Stanford Univ., Stanford, CA, June 2004.

[10]Nagarajan, S., Lele, S. K., and Ferziger, J. H., "A Robust High-Order Compact Method for Large Eddy Simulation," *Journal of Computational Physics*, Vol. 191, No. 2, 2003, pp. 392–419.

[11]Roach, P. E., and Brierley, D. H., "The Influence of a Turbulet Free-Stream on Zero Pressure Gradient Transitional Boundary Layer Development Part 1: Test Cases T3A and T3B," *Numerical Simulation of Unsteady Flows and Transition to Turbulence*, edited by O. Pironneau, W. Rodi, I. L. Ryhming, A. M. Savill, and T. V. Truong, Cambridge Univ. Press, Cambridge, England, U.K., 1992, pp. 319–347.

P. Givi
Associate Editor